AL/CF-TR-1997-0102

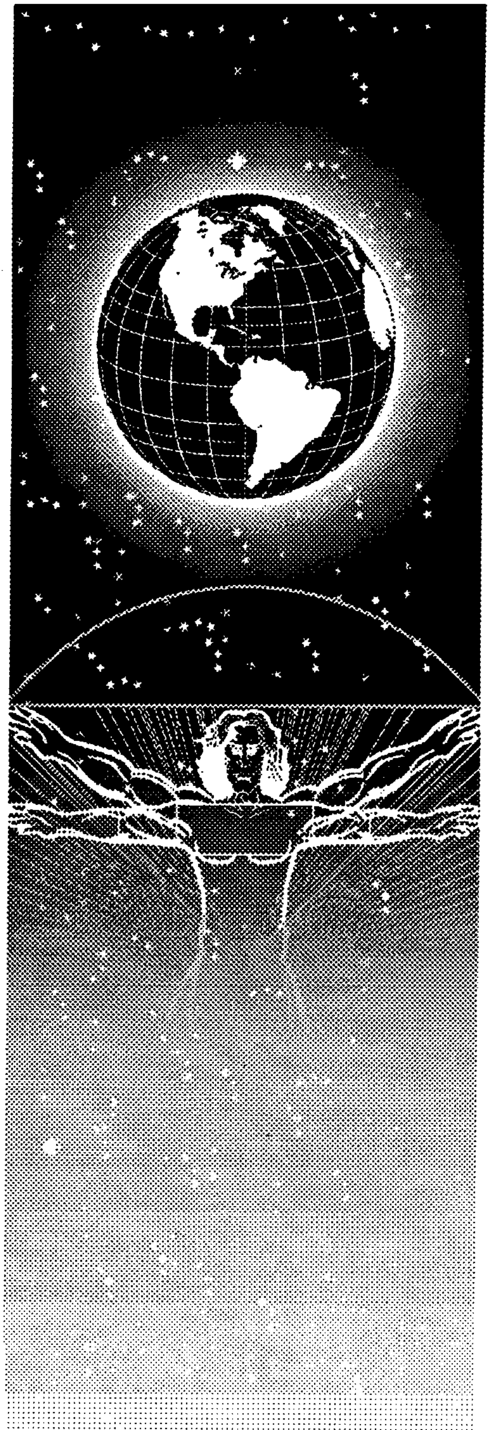

UNITED STATES AIR FORCE
ARMSTRONG LABORATORY

The Development of Auditory Icons for Representation of Virtual Objects in 3-D Space

Don C. Teas

DYNASTAT
2704 Rio Grande Suite 4
Austin TX 78705

December 1994

Final Report for the Period May 1994 to November 1994

Approved for public release; distribution is unlimited

Crew Systems Directorate
Biodynamics and
Biocommunications Division
Wright-Patterson AFB OH
45433-7901

NOTICES

DISCLAIMER

This Technical Report is published as received and has not been edited by the technical editing staff of Armstrong Laboratory.

TECHNICAL REVIEW AND APPROVAL

AL/CF-TR-1997-0102

The voluntary informed consent of the subjects used in this research was obtained as required by Air Force Instruction 40-402.

This report has been reviewed by the Office of Public Affairs (PA) and is releasable to the National Technical Information Service (NTIS). At NTIS, it will be available to the general public, including foreign nations.

This technical report has been reviewed and is approved for publication.

FOR THE COMMANDER

Thomas J. Moore

THOMAS J. MOORE, Chief
Biodynamics and Biocommunications Division
Crew Systems Directorate
Armstrong Laboratory

REPORT DOCUMENTATION PAGE

Form Approved
OMB No. 0704-0188

1. AGENCY USE ONLY *(Leave blank)*

2. REPORT DATE
December 1994

3. REPORT TYPE AND DATES COVERED
Final - May 1994 to November 1994

4. TITLE AND SUBTITLE
The Development of Auditory Icons for Representation of Virtual Objects in 3-D Space

5. FUNDING NUMBERS
C - F41624-94-C-6006
PE - 65502F
PR - 3005
TA - CB
WU - 4C

6. AUTHOR(S)
Don C. Teas

7. PERFORMING ORGANIZATION NAME(S) AND ADDRESS(ES)
Dynastat, Inc.
2704 Rio Grande Suite 4
Austin TX 78705

8. PERFORMING ORGANIZATION REPORT NUMBER

9. SPONSORING/MONITORING AGENCY NAME(S) AND ADDRESS(ES)
Armstrong Laboratory, Crew Systems Directorate
Biodynamics and Biocommunications Division
Human Systems Center
Air Force Materiel Command
Wright-Patterson AFB OH 45433-7901

10. SPONSORING/MONITORING AGENCY REPORT NUMBER
AL/CF-TR-1997-0102

11. SUPPLEMENTARY NOTES

12a. DISTRIBUTION/AVAILABILITY STATEMENT
Approved for public release; distribution is unlimited

12b. DISTRIBUTION CODE

13. ABSTRACT *(Maximum 200 words)*
Recent technology has enabled directional audio displays to be fielded in the cockpit. Directional audio displays convey the location of a sound source to the pilot. If a sound is chosen to indicate a certain event, qualitative data can also be communicated. This study examined several types of auditory signals, or icons, for use in the cockpit. Each of five icons was evaluated for five subjects' ability to localize and identify the icon. Spectral and temporal characteristics were varied among the icons. Three elevations were used for each of seven azimuth locations. Identification was nearly perfect for all icons while localization accuracy was highly variable. Both spectral and temporal features proved to be important for localization accuracy. Differences between subjects in elevation accuracy may be reduced by using custom head-related transfer functions. These findings are directly applicable to the design of auditory icons for use in directional auditory displays to be fielded in the near future.

14. SUBJECT TERMS
Icons Localization Virtual audio

15. NUMBER OF PAGES
39

16. PRICE CODE

17. SECURITY CLASSIFICATION OF REPORT	18. SECURITY CLASSIFICATION OF THIS PAGE	19. SECURITY CLASSIFICATION OF ABSTRACT	20. LIMITATION OF ABSTRACT
UNCLASSIFIED	UNCLASSIFIED	UNCLASSIFIED	UNLIMITED

NSN 7540-01-280-5500

Standard Form 298 (Rev. 2-89)
Prescribed by ANSI Std. Z39-18
298-102

This page intentionally left blank.

TABLE OF CONTENTS

LIST OF FIGURES

LIST OF TABLES

This page intentionally left blank.

1.0 IDENTIFICATION OF THE PROBLEM

Two sensory systems, vision and hearing, provide the flow of information that allows us to move safely in an environment filled with stationary and moving objects. From that flow of visual data not only can we avoid collision with an object, we also can know whether to step aside or run. So long as visibility is clear, that flow of visual data allows pilots in high speed aircraft to avoid collisions, however, they may fail to recognize events outside their visual field even though indicated by head-down radar. Recent technology has enabled us to provide similar information acoustically, making it possible to detect the location of objects outside the visual field and to move the eyes directly to the location of the acoustic event, thus reducing the eye movement normally involved in search and detect activities. Time spent in visual search is not well-used since we are effectively blind when the eyes are moving. If an event in space can be electronically detected, it can then be converted to an acoustic representation, the acoustic representation passed through transfer functions and the transformed acoustic data, now carrying information conveying source location, presented to a listener over earphones. As the listener turns his head to gaze at the object, the head-tracking devices maintain the object's position with respect to the listener in real time. The transfer functions capture the acoustic patterns at each ear that are representative of a sound source at a given location, thus providing the listener with spatial information. If the sound is chosen to indicate the kind of event that occurred, then both spatial and qualitative (i.e., identification) data about the event can be communicated to the listener. For example, the nature of the object, hostile or friendly, might be captured in the timbre of the sound. The receiver can benefit because the detection of an acoustic event, unlike detection of a visual event, is independent of head orientation -- the listener can observe an acoustic event while his gaze is directed elsewhere. Thus, the pilot can acoustically recognize both the location and quality of a specific event in space surrounding an aircraft while gazing at a head-mounted display and know whether to initiate an evasive maneuver. Our objective is to create effective acoustic icons for the use of pilots.

2.0 TECHNICAL OBJECTIVES

The technical objective of this effort was to conduct a feasibility study on the ability of listeners to localize certain auditory stimuli in virtual auditory space. The questions to be addressed as part of the study were as follows:

1. Does the accuracy of localization vary with the auditory icon?
2. Do the auditory icons vary in their identifiability?
3. Do the auditory icons elicit judgements which vary in confidence?
4. Is the identifiability of an icon related to error of localization?
5. Is the confidence in a localization response for an icon at a virtual location related to its identifiability?
6. Is localization error related to confidence in the localization judgement?
7. Is there an interaction between icon and confidence in the lateralization judgement for virtual angles? (One might expect that all the icons would elicit secure judgements at 0°,0° but at lateral positions, some icons may elicit more secure judgements than others.)

3.0 WORK PERFORMED

In the Phase I effort five acoustic icons were generated and presented to listeners and the listener's performance in attributing a spatial location to them was measured. Each listener responded by orienting their head, i.e., pointing their nose, toward the virtual sound source which varied randomly in both azimuth and elevation from trial to trial, with the restriction that the numbers of presentations among the categories of azimuth and elevation be equal within a tolerance limit. The head-orientation made by each listener was read from the head-tracker and used as an indication of the location of the virtual source on that trial. These locations were analyzed using statistics that recognized the listener's location as the center of a sphere and the head orientations as vectors. The procedures used for the assessing the central tendency and variability of the judgements, i.e., head orientations, are described in the Appendix B.

The icons were generated with LabVIEW, a graphic programming language suitable for a number of applications. The spectrum and time waveforms for the five icons are shown in Figs. 1 to 5. All signals were 250 msec in duration and were repeated. Subjects varied in their need for repetitions. In training, some listeners wanted the signal repetitions to continue after they had approximated the direction of the virtual source so that a confirmation could be obtained. Other listeners were more secure in their head positioning. In the test runs, 10 signal repetitions were used for all listeners. A 50% duty cycle was used during the presentation of the icons so that the approximate duration of the stimulus was 5 sec. For some orientations, e.g., 135 or 225 degrees, the time required to reach the position and make a determination was longer than the five seconds for some listeners.

The listeners were chosen from about 15 applicants who responded to an advertisment in the university newspaper. One criterion was availability and the other was performance on a screening test to determine whether they could localize the noise burst, presented in the front half of the auditory field, i.e., between 90 and 270 degrees at the median plane greater than 70% of the time. The range of variation in correct judgements among the persons responding to the advertisement was from 20% to 94%. Six subjects were hired but one dropped out after 2 weeks of participation, leaving 5 listeners who completed the training and the test. Initially, there were three females and three males. We completed the study with three females and two males.

4.0 PROCEDURES

4.1. Icons

Figures 1 - 5 show graphic representation of the icons used in Phase I. The upper display in each panel represents the time waveform of the icon and the lower panel shows the spectrum. Fig. 1 represents the 500 Hz sine tone burst. The icon was stored as a file that the presentation program read. The displays shown here are from those files. The cursor is located at the peak of the spectrum shown in the bottom panel of Fig. 1. Fig. 2 shows the waveform and spectrum for the noise burst. The cursor is located at about 300 Hz, the low frequency cut-off for the noise. Figure 3 shows the waveform and spectrum for the icon labeled, Plses. The pulse rate was 500 Hz and the lower panel shows the spectrum with peaks spaced at 500 Hz. Figure 4 and 5 show the waveforms and spectra for the two sweep stimuli. Figure 4 represents the sweep from 300 Hz to 8 kHz. Figure 5 represents the sweep from 300 Hz to 1.5 kHz. Since the upper terminus is nearer the start for the 0.3 to 1.5 kHz sweep, the duration of the lower frequencies is greater than for the 0.3 to 8 kHz sweep and the time waveform is a bit clearer. The pulses, noise burst and the 8k Sweep have spectral representation above 1000 Hz. The pulses and the noise burst

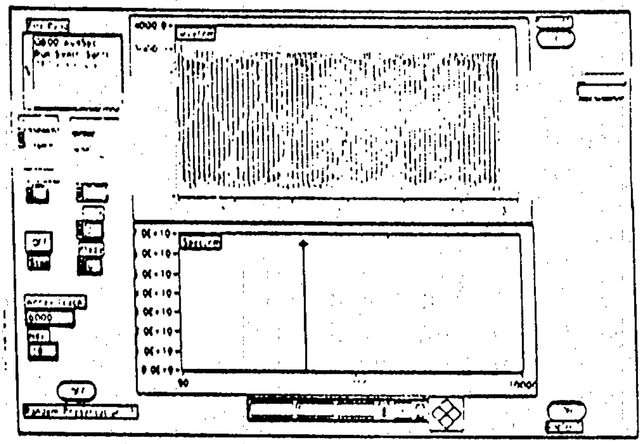

Figure 1. 500 Hz Tone Burst

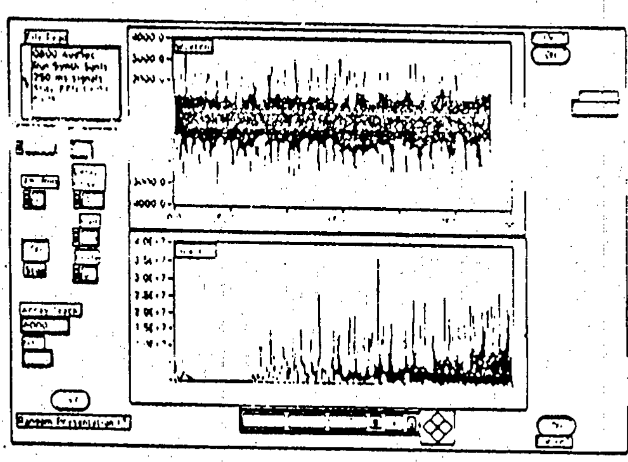

Figure 2. Noise Burst

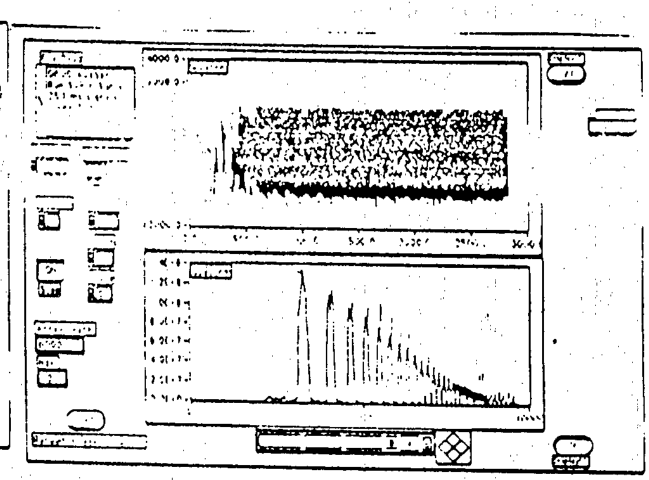

Figure 4. Sweep 300 - 8000 Hz

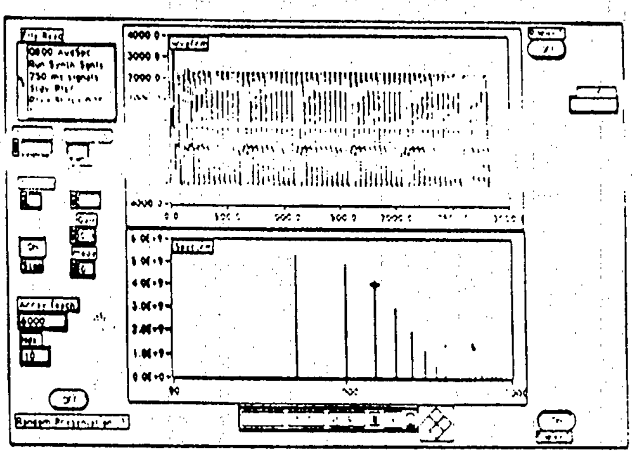

Figure 3. Pulses

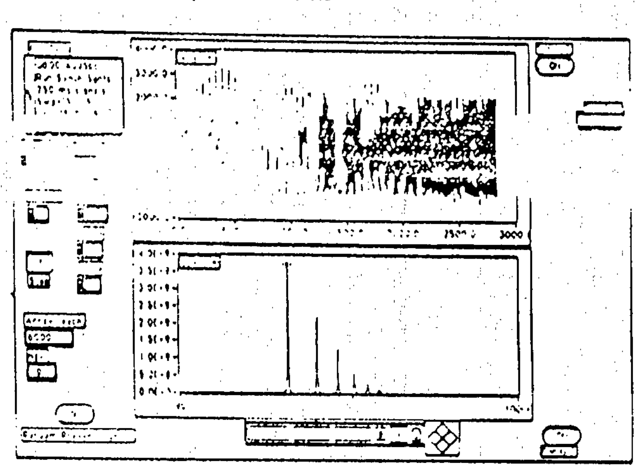

Figure 5. Sweep 300 - 1500 Hz

have strongest representation at the highest frequencies and thus, one can expect that elevation might be best perceived for these icons and less so for the tone burst and the 1.5 kHz Sweep. One subject, MP, had difficulty reporting the two sweep stimuli correctly, but also confused the 500 Hz sine with 1.5 kHz sweep stimulus.

4.2 Presentation

The presentation program, written with LabVIEW, contained selectors which chose, on a random basis, the azimuth, elevation and icon to be presented on a given trial. The icon was output, via a 16-bit D/A converter (National Instruments, A-2100) to the 3-D Audio Generator instrument from Systems Reseach Lab. Also output were the azimuth and elevation at which the icon was to be presented. After the presentation was completed, the program waited for the information from the head-tracker (Polhemus Iso-tracker), then stored it in a file, previously established for that listener and set of conditions. Each trial began with a zero-gaze to establish the reference for that trial. The signal was then presented and the listener oriented toward the virtual source. The head position was read and then the listener indicated identification of the target angle, the identification of the icon, and the confidence rating with a key on the number pad. Following the number-pad entry, the next trial began.

4.3 Training

All listeners received similar training experience. The initial exposure to the virtual sources was on the horizon at azimuths of 270, 315, 0, 45 and 90 degrees. Only the NBurst icon was used. The listeners became accustomed to the changes in the sounds presented through the earphones as they turned their head to orient toward the virtual source. It was during these trials that the listeners learned to point their nose at the sound and not their eyes. After satisfactory performance at these azimuths, locations at 135^0 and 225^0 were added. These locations required the listeners to turn their body toward the rear of the room in order to get the head orientation correct. The rotating stool was important for locating these azimuths.

As the performance of the listeners improved for the full range of azimuths, elevations were added to the sequence of randomly presented source locations. The head orientations to the elevations, 45^0 (above the horizon) and 135^0 (below the horizon) proved to be more difficult than to point at azimuths. The presentation program was modified so that the listeners could be informed about the elevation to be presented. This allowed them to relate the perception to the angle presented. The program could also inform the listener when the head orientation was correct. In this way, the listeners were trained with feedback. Following this training, carried out with the NBurst icon, the other icons were included in the trial sequence. In the test trials, for which the results are reported below, no information about the virtual source location was presented.

5.0 RESULTS

5.1 Category Judgments

5.1.1 Azimuth

Early in the course of the training, listeners were asked to indicate the location of the virtual source by striking a key on the number pad. Figure 6 shows the association between category numbers and the azimuth location. The number "1" was not used nor was it chosen as a virtual source. As previously reported listeners had little difficulty in the identification of azimuth location. This strategy was particularly helpful in encouraging the subject to turn the head rather than using eye movements to look at the virtual source. It also helped the experimenter to know that the perception of the location was better than the head orientation indicated, particularly at the beginning of training for the listeners. Table I shows the relative probabilities for assigning categories to the azimuth positions.

5.1.2 Identification

The listeners had little difficulty in identifying the icons as they were presented. By the second day of exposure to the five icons, identification was highly accurate. The listener's instructions were to associate the NBurst with the numeral "1", the 8kSweep with "2", the TBurst with "3", the 1.5 kSweep with "4", and the Pulses with "5". The transition from using the number pad for azimuth "name" to using it for icon "name" was practically immediate. Table II shows the matrices for the identifications made by each listener.

5.1.3 Confidence Ratings.

The use of the confidence intervals by the listeners was not very informative. The numbers were not used well, i.e., the listeners tended to use the middle range most frequently and not to differentiate among the full range. The data from one listener were analyzed in some detail, particularly with respect to whether poor confidence ratings correlated with front-to-back reversals and there was some indication that this was the case. However, the number of reversals for the other listeners was not great enough to test that relation.

5.1.4 Ancillary Data.

Two additional sets of data were obtained on the listeners. They self-administered a LabVIEW-based audiogram and they also visited the University of Texas Speech Science Dept. to have impedance measurements of the left and right ears made and evoked acoustic emission recorded and analyzed. Table III shows the decibels (re one millivolt) for the audiograms. (Note: the audiograms were self-administered in a quiet office). The greatest interaural difference was 5 dB for listener AT. This listener performed poorly for elevation and some azimuths, however, listener RK, the best-performing subject, showed a 4 dB difference, also at 4 kHz. The evoked emissions showed some upper frequency differences for both listeners. Ear molds were made of each subject, however, we have not yet attempted to carry out an analysis of what appear to be substantial differences among them.

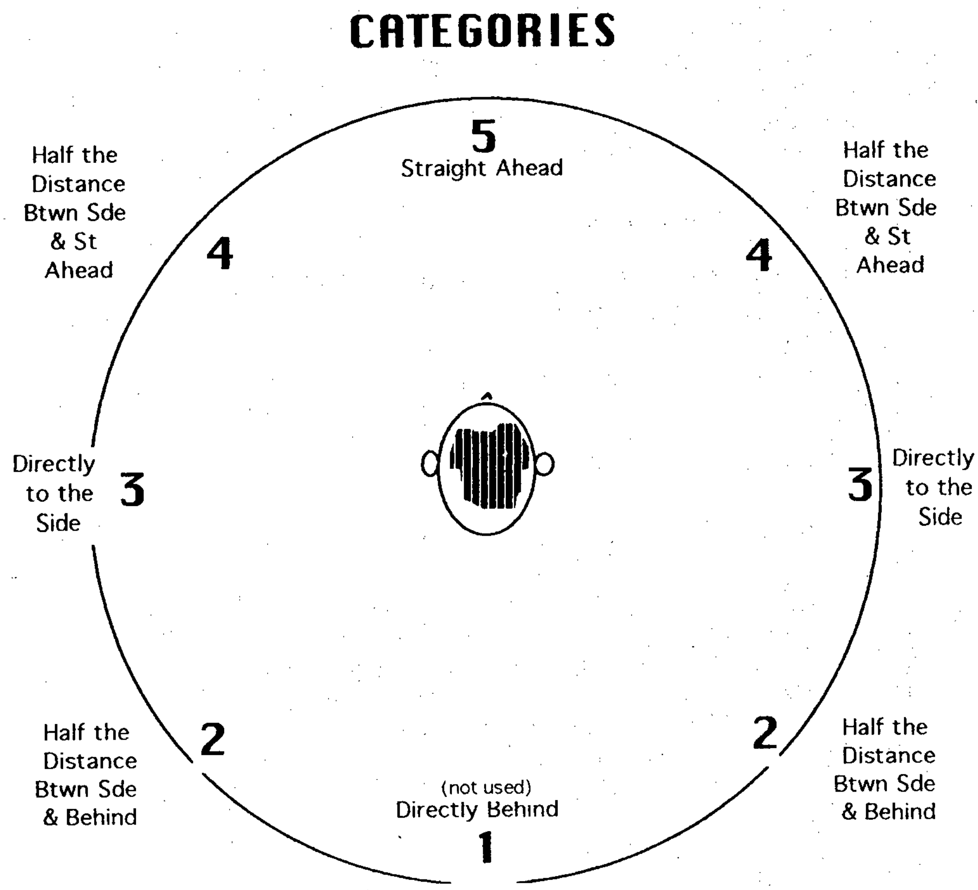

Figure 6. Category Judgement

RELATIVE PROBABILITIES FOR CATEGORY ASSIGNMENTS (1 week)							
Degrees							
	0	45	90	135	225	270	315
Listeners							
rk	1	0.93	0.9	1	1	0.9	0.93
kb	1	1	1	0.8	0.6	0.4	1
mp	0.9	0.85	1	0.9	0.9	0.7	0.73
at	0.9	0.8	0.9	0.9	1	0.7	0.93
bw	0.9	0.6	0.9	1	1	0.9	0.87

Table I. Relative Probabilities for Category Assignment

kb 10/3/94 (E1,5)

Response#

Signal#	*0*	*1*	*2*	*3*	*4*	sum
0 (noise burst)	22	0	0	0	0	22
1(Swp 0.3-8k)	0	19	1	1	0	21
2 (.5k burst)	0	0	21	0	0	21
3 (Swp .3-1.5k)	0	0	0	21	0	21
4 (Pulses .5k)	0	0	0	0	21	21

mp 10/3/94 (E1,5)

	0	*1*	*2*	*3*	*4*	sum
0	21	0	0	0	0	21
1	0	10	0	10	0	20
2	0	0	0	20	1	21
3	0	6	1	12	0	19
4	0	0	1	0	16	17

kb 10/5/94 (E2,1)

Response#

Signal#	*0*	*1*	*2*	*3*	*4*	sum
0 (noise burst)	22	0	0	0	0	22
1 (Swp .3-8k)	0	21	0	0	0	21
2 (.5k burst)	0	0	21	0	0	21
3 (Swp .3-1.5k)	0	1	1	21	5	21
4 (Pulses-.5 k)	0	0	0	0	21	21

mp 10/5/94 (E2,1)

	0	*1*	*2*	*3*	*4*	sum
0	21	0	0	0	0	21
1	0	15	2	2	0	19
2	0	0	21	0	0	21
3	0	1	0	20	0	21
4	0	0	1	0	17	18

rk 10/4/94 (E1,3)

	0	*1*	*2*	*3*	*4*	sum
0 (noise burst)	22	0	0	0	0	22
1 (Swp .3-8k)	0	20	1	0	0	21
2 (.5k burst)	0	0	21	0	0	21
3 (Swp .3-1.5k)	0	0	0	20	1	21
4 (Pulses	0	2	0	0	19	21

at 10/3/94 (E1,5)

	0	*1*	*2*	*3*	*4*	sum
0(noise burst)	22	0	0	0	0	22
1(Swp .3-8k)	0	20	0	1	0	21
2(.5k burst)	0	1	20	0	0	21
3(Swp .3-1.5k)	3	0	0	18	0	21
4(Pulses .5k)	0	0	0	0	18	18

wb 10/3/94 (E1,5)

	0	*1*	*2*	*3*	*4*	sum
0	21	0	0	0	0	21
1	0	21	0	0	0	21
2	0	0	20	0	1	21
3	0	0	0	21	0	21
4	0	0	1	1	18	20

at 10/7/94 (E3,1)

	0	*1*	*2*	*3*	*4*	sum
0(noise burst)	21	0	0	0	1	22
1(Swp .3-8k)	1	18	1	1	0	21
2(.5k burst)	0	0	21	0	0	21
3(Swp .3-1.5k)	0	1	0	19	1	21
4(Pulses .5k)	0	0	0	0	19	19

wb 10/5/94 (E2,1)

	0	*1*	*2*	*3*	*4*	sum
0	21	0	0	0	0	21
1	0	21	0	0	0	21
2	0	0	21	0	0	21
3	0	0	0	20	0	20
4	0	0	0	0	21	21

Table II. Identification (Confusion Matrix)

Listener	rk		kb		mp		at		bw	
	Lft	Rght	Lft	Rght	Lft	Rght	Lft	Rght	Lft	Rght
Volume(cc)	0.7	0.9	0.9	0.8	1.6	1.7	0.7	0.5	1.0	1.0
Hearing Level	(dB re 1 mv)									
Frequency										
250	60	61	62	69	71	34	69	65	44	46
500	48	48	55	60	58	49	53	52	37	37
1000	38	38	35	34	35	34	35	34	35	35
2000	38	35	35	35	35	34	35	35	35	35
3000	38	34	35	34	34	34	35	34	35	34
4000	44	40	35	35	35	35	47	42	40	37

Table III. Canal Volume and Hearing Level

The data for localization, i.e., head-pointing, are summarized in Figs. 7 through 11 and show the performance of each listener on the three test trials (The tables with the raw data used to construct these figures are given in Appendix A). Figures 7.1a - 11.1a show the relation between the azimuth angles averaged over the three elevations and the three runs. Each data point includes six values. The angle, 180^0, is included in order to keep the slope of the relation between judged and presented angles at 1.0, indicated by the arrow added to the panel. Figures 7.1b - 11.1b show the average error in elevation judgements, summed across azimuth angles. Each point includes 21 values (seven azimuth angles and three runs). Below Panel B the tables show the values represented graphically in the panels. Figures 7.2a-c to 11.2a-c shows the vector angle of error for azimuth at each elevation and Figures 7.2d-f to 11.2d-f show the dispersion for the vector angle of error.

The average azimuth responses were more accurate than the average elevation responses. This result supports the results from the category judgements of the perceived azimuth angle. At the time of the test runs, the frequency of occurrance of reversals had decreased considerably. For the two most accurate listeners (Figs. 7.1a and 8.1a) the average azimuth localization was practically independent of icon. For the remaining listeners, the differences among icons was larger, but still not very great . Listener BW (Fig. 11.1a) was small in stature and probably her pinnae were much smaller than the pinnae on which the Head Related Transfer Functions were based. The most accurate subject (RK, Fig. 7.1a) was the tallest of the five listeners. However, I know of no anthropometric data that relate height to pinna size. The three less accurate listeners also showed a larger azimuth error at 315^0, i.e., 45^0 left of center, than the two more accurate listeners.

The average elevation responses show a bias toward 135^0, i.e., 45^0 down, toward earth, when the stimulus was presented at 90^0, i.e., horizontal. Three listeners (Figs. 9.1b -11.1b) agreed closely with the horizontal presentation, and one other (Fig. 8.1b) showed a single aberrant point for the 8kSweep icon. Four of the five listeners responded to the TBurst icon with a more extreme value, i.e., with an error between 40 and 50 degrees. In general, elevation responses showed large errors.

5.1.5 Angle of Error

The angle of error and κ^{-1} were calculated with the procedures described in Appendix B. These figures are derived from spherical coordinates in which azimuth and elevation angles are considered together rather than separately, i.e., x (for azimuth) and y (for elevation) coordinates. The use of spherical coordinates does not require the assumption that azimuth and elevation errors are independent, but considers the response as a direction indicator. A direction can be consistently deviant from the target, indicating that the perception of direction was due to a systematic error, in which case κ^{-1} would be small. Conversely, a calculated angle of error could be due to wide variation across the three runs, in which case κ^{-1} would be large, indicating that the listener was inconsistent in the perception of target location. The two measures are used together.

Inspection of Figs. 7.2a-f to 11.2a-f for each of the five listeners shows that the two measures can vary independently. For example, the κ^{-1} figures for listener RK showed a high consistency for localizations of the NBurst and the Pulses icons and great inconsistency in the localizations for the 8 kHz Sweep icon. In this example, the angle of error for the 8 kHz Sweep icon was large, i.e., the two measures varied together. Localizations for the other icons, TBurst and 1.5k Sweep, also showed large angles of error and variability. For listener MP, Figs. 9.2a and 9.2d, however, the dispersion at 45^{-} elevation was small, but the angle of error was large. Some target angles were less accurately localized than others. In particular, responses to the target angle at 315^{-} were most variable for all three elevations. Among the three elevations, the most variable was 45^{-}, above the horizon. The elevation below the horizon, at 135^{-}, was the least variable.

The greatest dispersion among subjects was found for listener AT, Fig. 10.2a, in the responses to 45^0 elevation. The data suggest that this listener did not discriminate the elevation angle. Best performance was for the 135^0 elevation for azimuths less than 90^0, a rather restricted range of capability. For the latter angles, the consistency of responses was fairly good, indicating that the perceptions repeated for repeated presentations of those conditions. Listener MP , Fig. 9.2a-c, showed good consistency in the responses, but showed notable peaks of inconsistency at 315^0 and 135^0 azimuth, and the angles of error, particularly for 45^0 elevation, were substantial. This combination suggests that the perceptions were stable, but for the noted exceptions. Listener KB, Fig. 8.2a-f, was most consistent for the elevation at 90^0, and even there showed some extremes, but showed large variability at the two elevations. However, the angles of error for the two elevations were smaller than for some of the other listeners. Listener BW, Fig. 11.2a-f, was also variable in her responses, but showed particular regions of uncertainty more clearly than some of the other listeners. The data show that listeners had particular difficulty at an azimuth of 225^0 at the 45^0 and the 135^0 elevations. Both the angle of error and κ^{-1} are large for this listener, indicating great uncertainty about the perception of the target at that location.

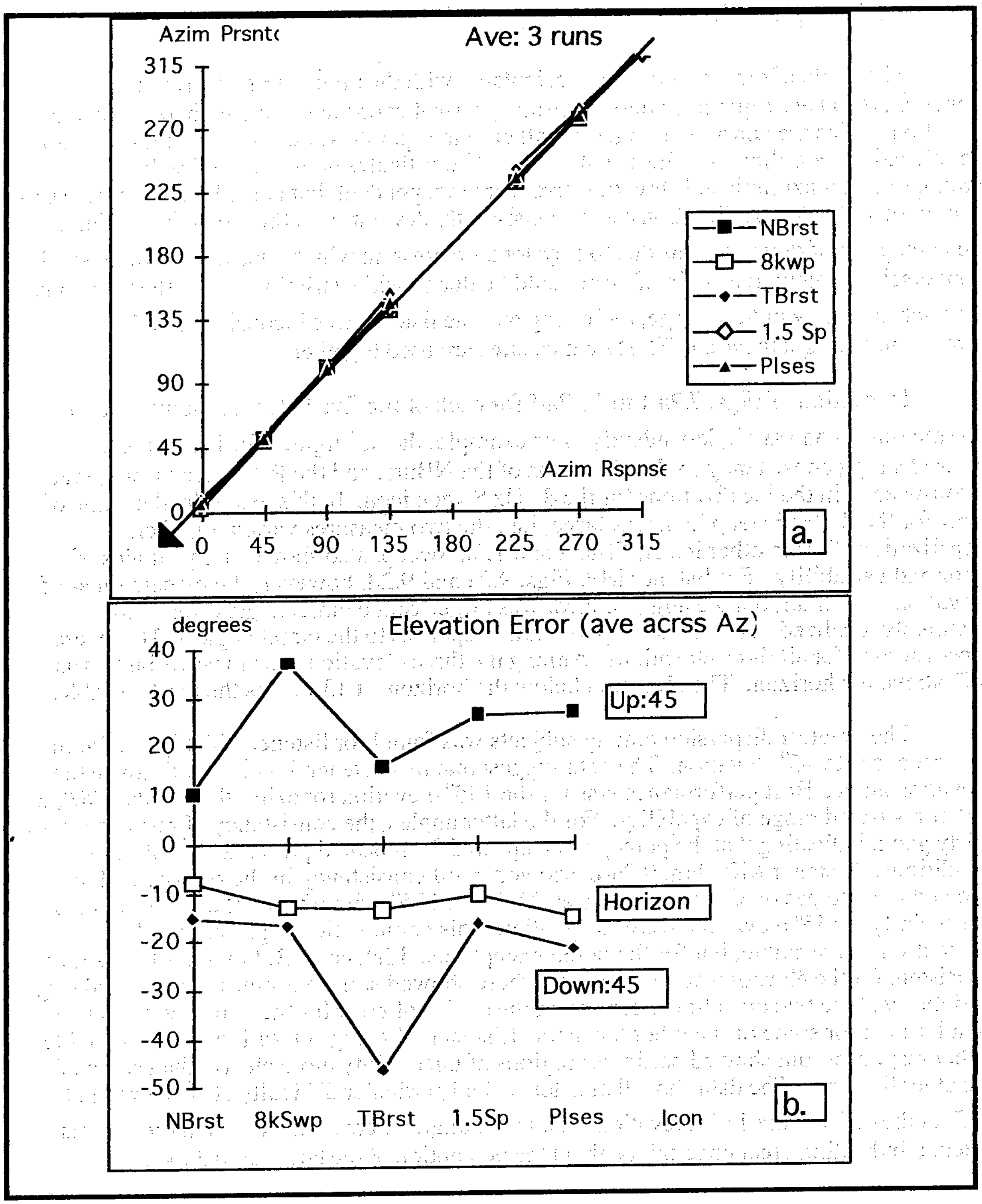

Fig. 7.1a. Average Response Across Elevation (Listener RK - 3 runs)
Fig. 7.1b. Average Error Across Azimuth (Listener RK - 3runs)

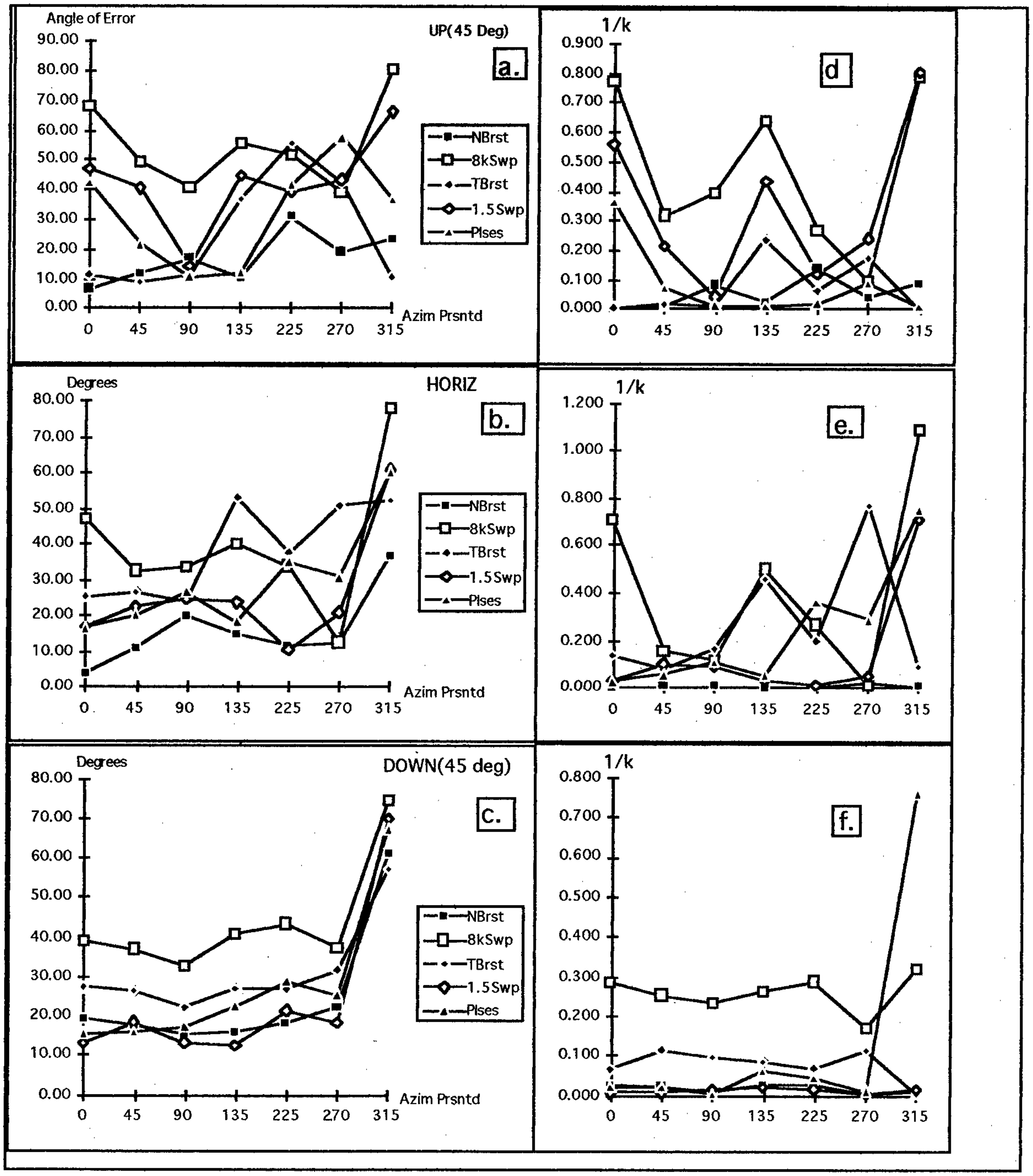

Fig. 7.2a-c. Vector Angle of Error Across Azimuth (Listener RK)
Fig. 7.2d-f κ^{-1} (Variability) Across Azimuth (Listener RK)

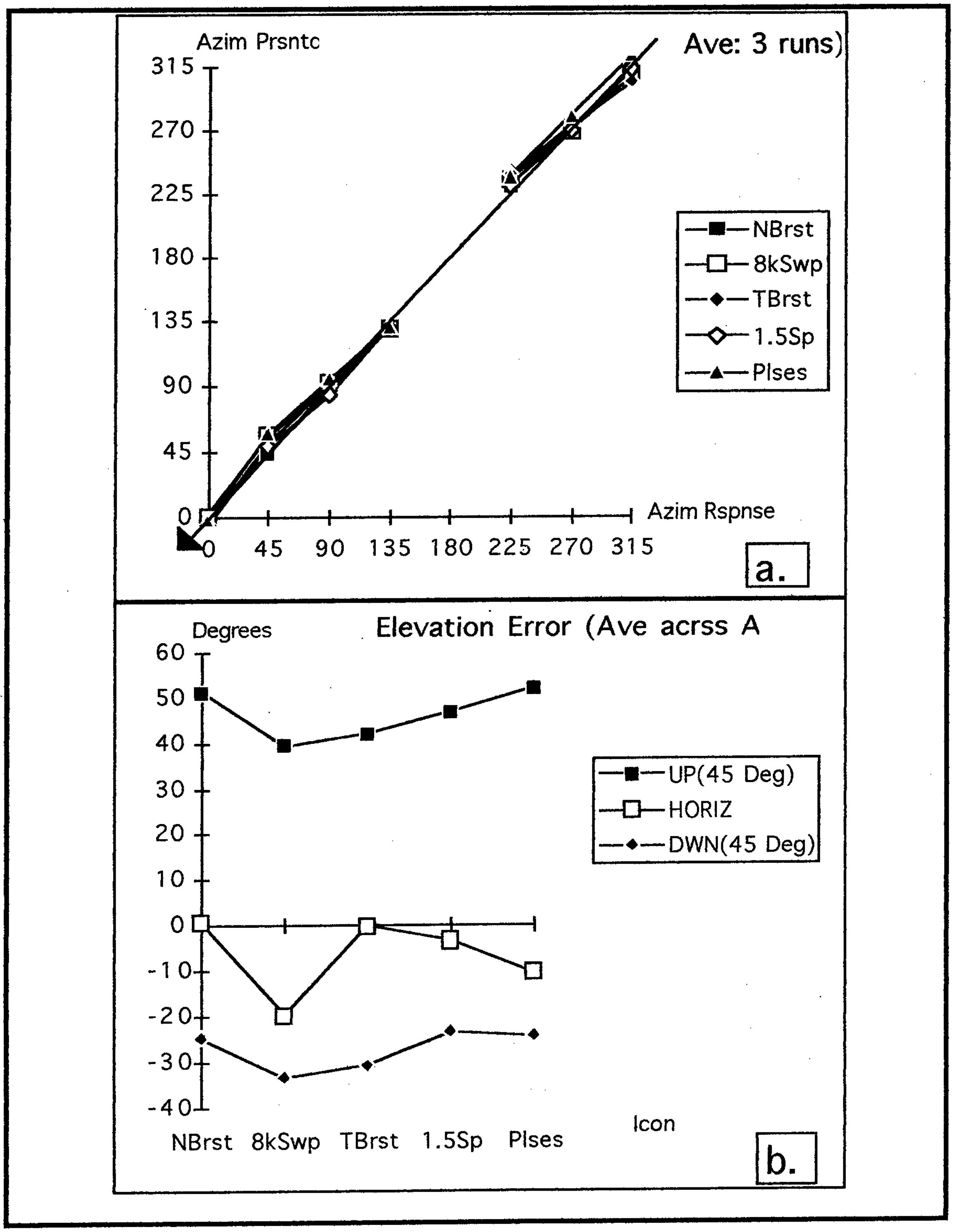

Fig. 8.1a. Average Response Across Elevation (Listener KB - 3 runs)
Fig. 8.1b. Average Error Across Azimuth (Listener KB - 3runs

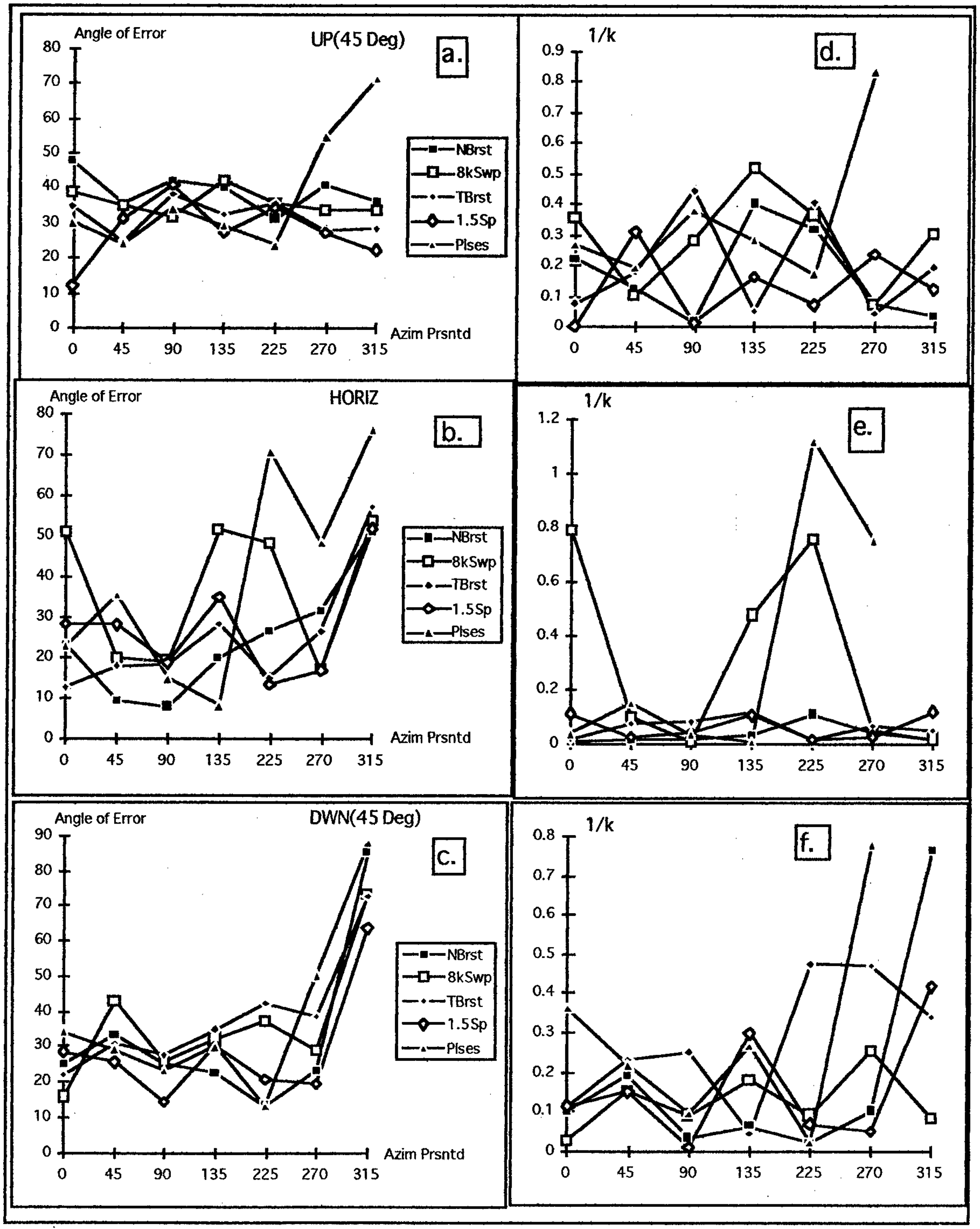

Fig. 8.2a-c. Vector Angle of Error Across Azimuth (Listener KB)
Fig. 8.2d-f κ^{-1} (Variability) Across Azimuth (Listener KB)

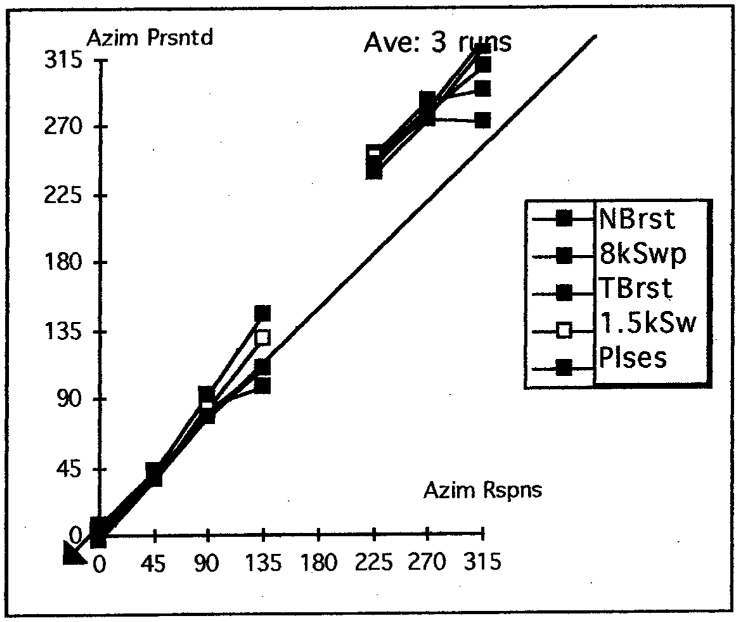

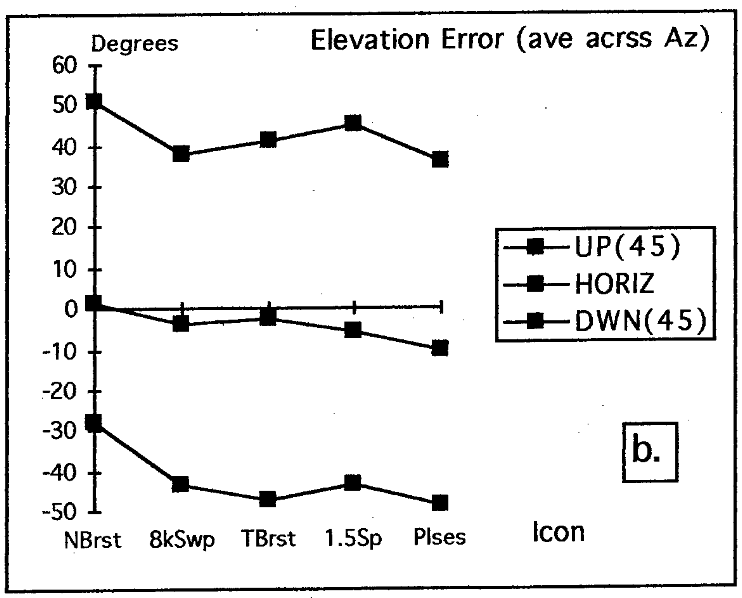

Fig. 9.1a. Average Response Across Elevation (Listener MP - 3 runs)
Fig. 9.1b. Average Error Across Azimuth (Listener MP)

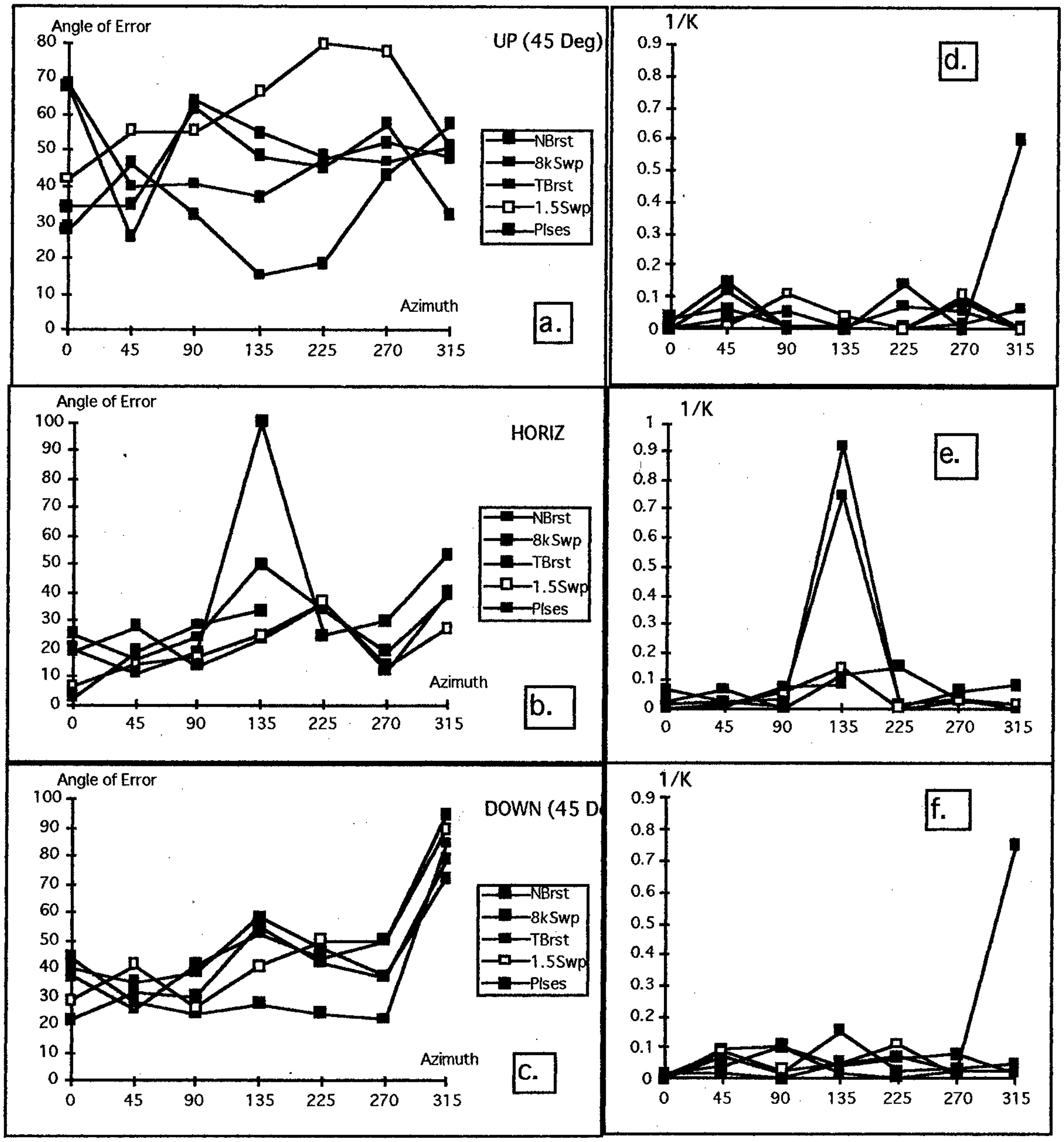

Fig. 9.2a-c. Vector Angle of Error Across Azimuth (Listener MP)
Fig. 9.2d-f. κ^{-1} (Variability) Across Azimuth (Listener MP)

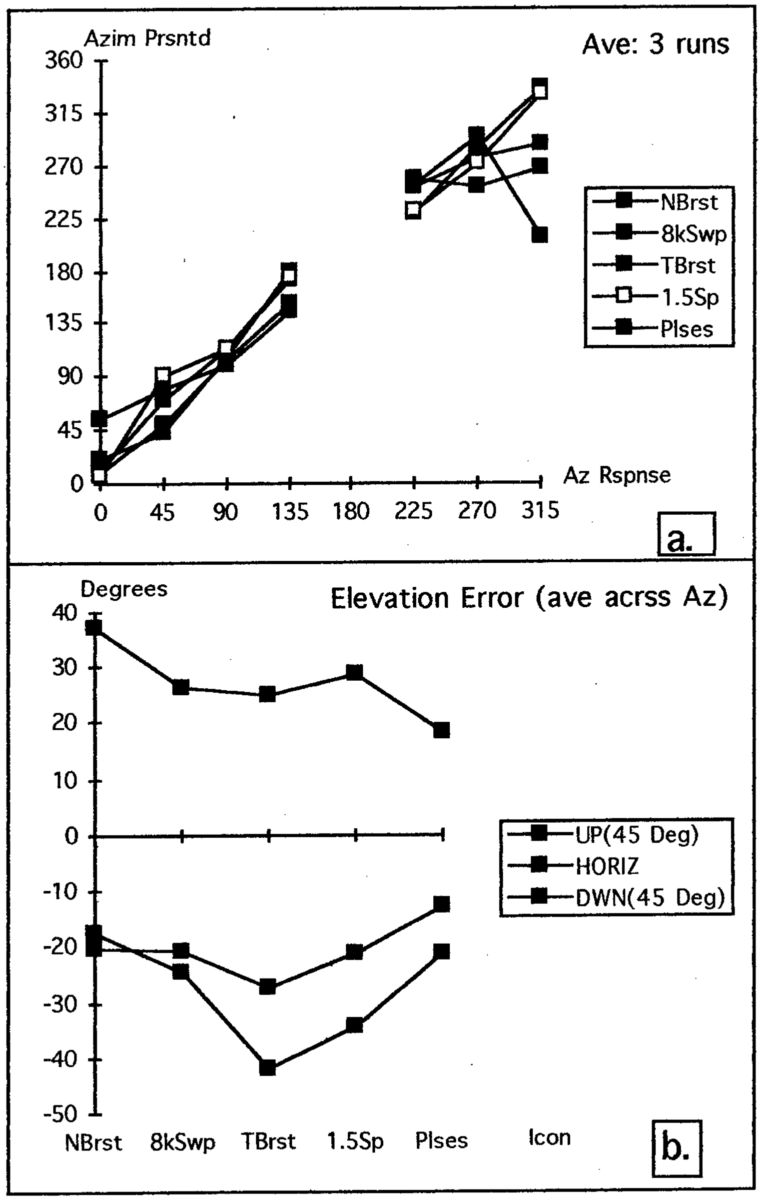

Fig. 10.1a. Average Response Across Elevation (Listener AT - 3 runs)
Fig. 10.1b. Average Error Across Azimuth (Listener AT - 3runs)

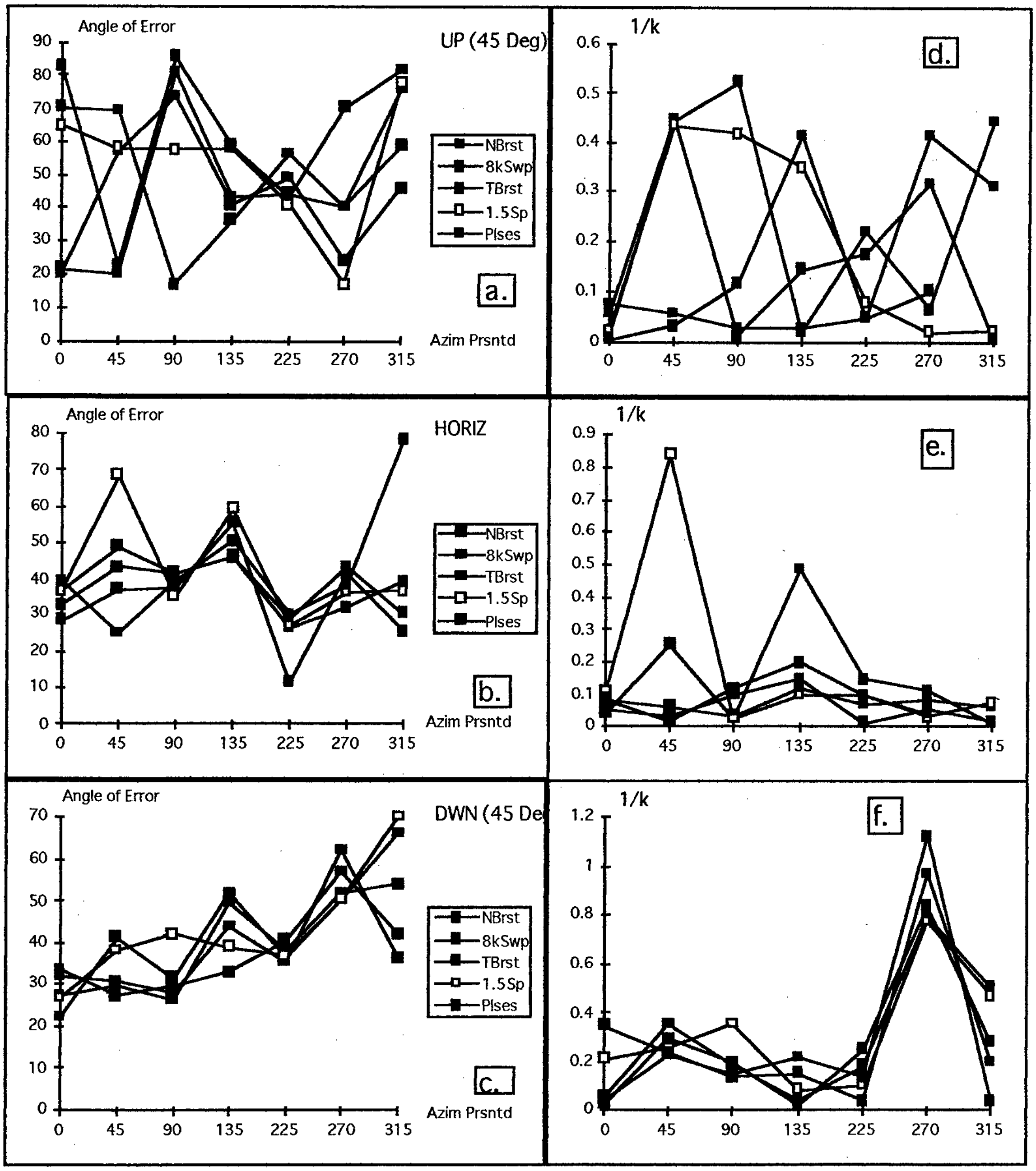

Fig. 10.2a-c. Vector Angle of Error Across Azimuth (Listener AT)
Fig. 10.2d-f κ^{-1} (Variability) Across Azimuth (Listener AT)

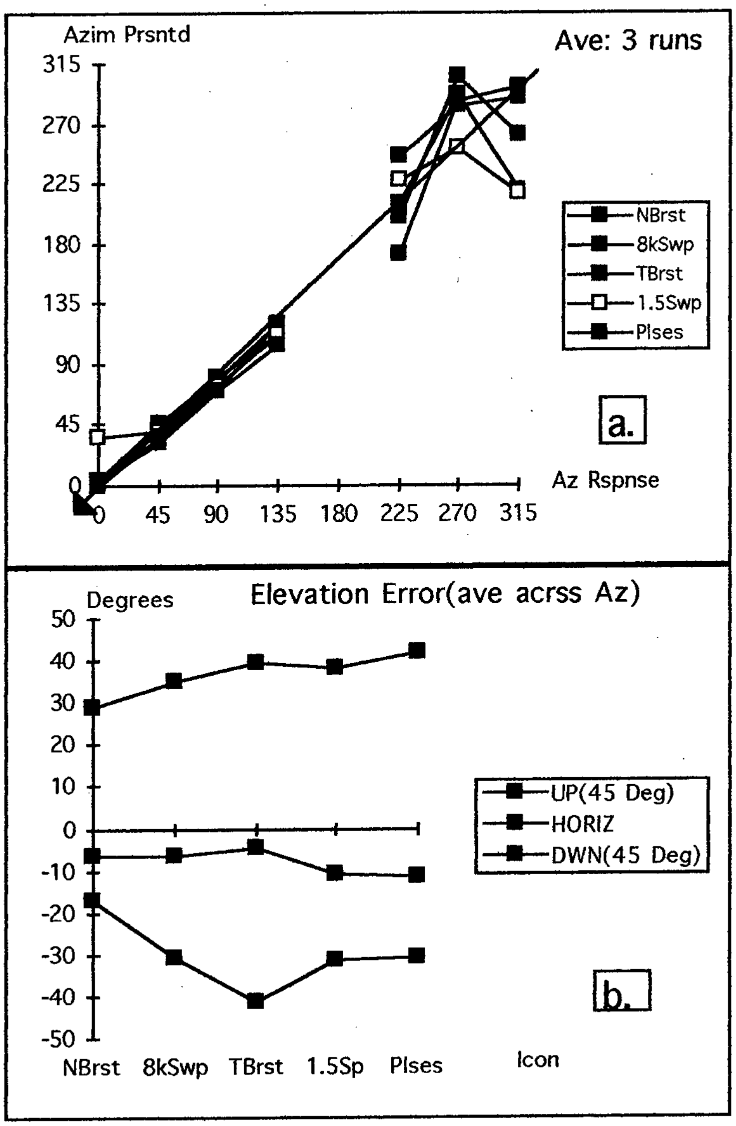

Fig. 11.1a. Average Response Across Elevation (Listener BW - 3 runs)
Fig. 11.1b. Average Error Across Azimuth (Listener BW - 3runs)

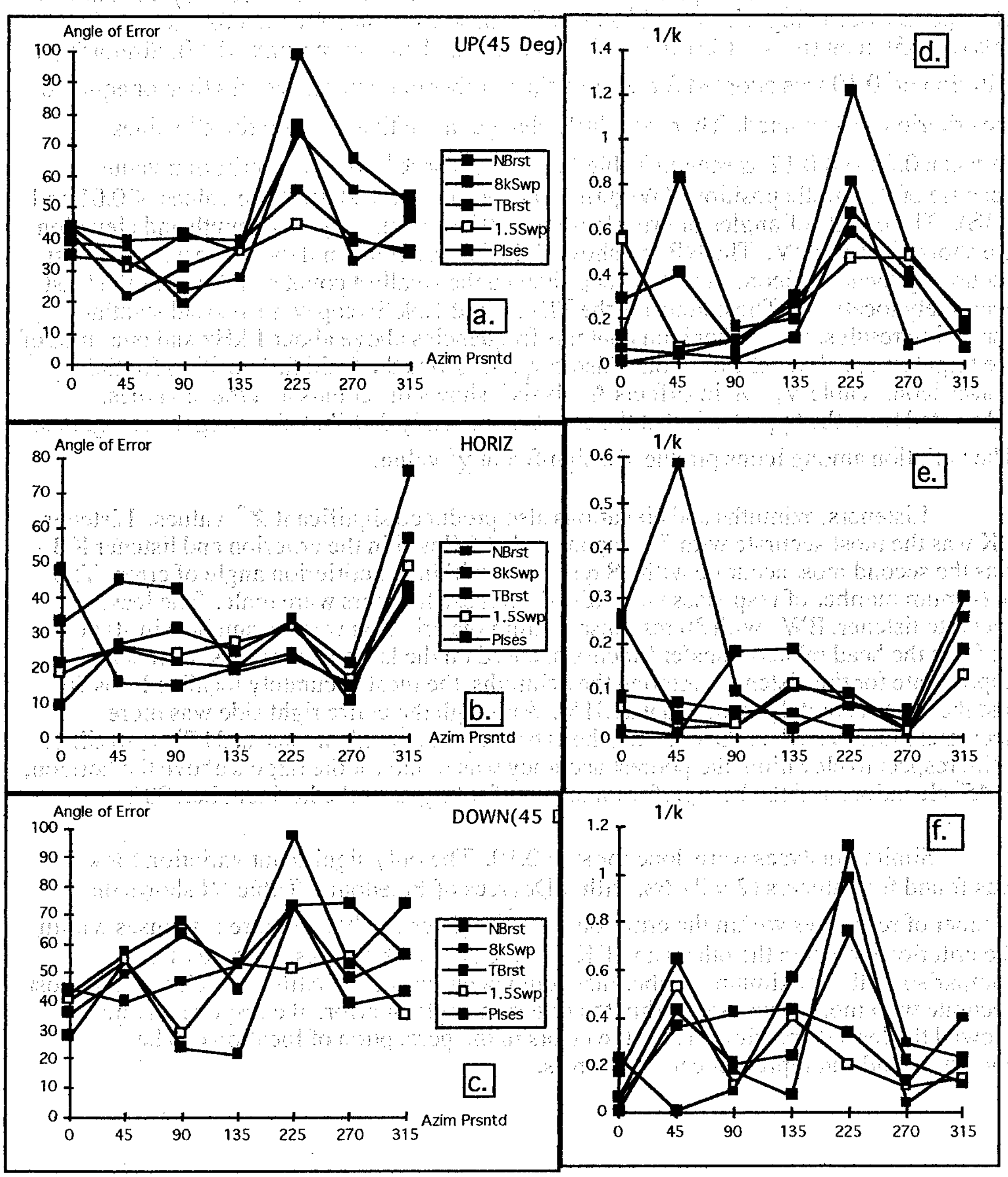

Fig. 11.2a-c. Vector Angle of Error Across Azimuth (Listener BW)
Fig. 11.2d-f κ^{-1} (Variability) Across Azimuth (Listener BW)

In order to assess the performance of the listeners more systematically, the number of responses occurring within a 30^0 angle of error was counted for each listener (max.=105), icon (max.=105), azimuth (max=75) and elevation (max.=175). Similarly, a criterion of 0.10 was adopted for κ^{-1} and the number of occurrances less then or equal to the criterion was counted. There was little change in relative position for κ^{-1} values between 0.08 and 0.12 as seen in Table IV. We chose κ^{-1} =0.10 as a criterion value because of its middle position. (Wightman and Kistler (1989) illustrate values of 0.01 and 0.18). The counts of angles of error less than 30^0 for icon, subject, azimuth and elevation are shown in Table IV. The NBurst showed the largest count and therefore was the most accurately localized icon. The 8k Sweep showed the smallest count and thus was the least accurately localized. The counts for the TBurst and 1.5k Sweep were also substantial, a surprising result since neither icon contains frequencies above about 1 kHz and one-third of the targets were above the horizon. Also surprising was the "middle" position for the Pulses icon. Table V, "Main Effects Analysis", shows the counts and the 2 values, calculated from the hypothesis that the counts are equally distributed among the categories. The variation among Icons produced a significant χ^2 value.

Listeners, azimuths and elevations also produced significant χ^2 values. Listener RK was the most accurate with 57 responses that fell within the criterion and listener KB was the second most accurate with 48 responses within the critierion angle of error. The maximum number of responses was 105. Both these listeners were male. The least accurate listener, BW , with 30 responses within the criterion was the smallest in stature. Perhaps the head related transfer functions, based on the large Kemar ears, were least appropriate for this listener. Among the azimuths, the most accurately localized was 90^0 and the least accurately localized was 315^0. Although the entire right side was more accurately localized than the left side, the extremely poor performance at 315^0 is puzzling. With respect to elevation, the poorest accuracy was found for the targets above the horizon, at 45^0 elevation, and the best performance was for targets at the horizon, i.e., 90^0.

Similar analyses were done for κ^{-1}= 0.10. The only significant variation for κ^{-1} was found for listeners (2 = 21.68, with 4 Degrees of Freedom). Table VI shows the number of responses within the criterion for κ^{-1}. Listener MP had more responses within the criterion (88) than the others and RK was the next with 63. As for the earlier comparisons, the maximum number that could occur was 105. Although RK was the most accurate with more responses within the criterion angle of error, the responses from MP showed the least dispersion. Thus, the errors in the perception of location can be consistent and can represent constant errors.

1/k<0.12	rk			kb			mp			at			bw			Acrss Subj's		
																SUM		
	45	90	135	45	90	135	45	90	135	45	90	135	45	90	135	45	90	135
NBrst	6	7	7	3	7	5	7	6	7	3	6	2	1	4	1	20	30	22
8k swp	1	2	0	2	4	4	6	6	7	3	7	2	5	5	0	17	24	13
TBrst	5	2	7	3	7	2	7	6	6	5	3	2	3	6	3	23	24	20
1.5Swp	2	6	7	3	7	4	7	6	7	4	6	2	2	6	3	18	31	23
Plses	6	4	6	0	3	2	4	5	6	4	4	1	3	4	1	17	20	16
sum	20	21	27	11	28	17	31	29	33	19	26	9	14	25	8			
																140	219	229

1/k<0.10	rk			kb			mp			at			bw			SUM		
	45	90	135	45	90	135	45	90	135	45	90	135	45	90	135	45	90	135
NBrst	6	7	7	3	6	3	7	6	6	3	6	2	1	4	1	20	29	19
8k swp	1	1	0	1	4	4	6	6	6	3	6	2	4	4	1	15	21	13
TBrst	5	2	5	3	6	1	7	5	6	5	3	2	3	6	3	23	22	17
1,5Swp	1	6	7	3	4	3	5	6	6	4	5	1	1	5	2	14	26	19
Plses	6	3	6	0	3	2	4	5	6	3	3	1	2	4	1	15	18	16
sum	19	19	25	10	23	13	29	28	30	18	23	8	11	23	8			
																132	206	219

1/k<0.08	rk			kb			mp			at			bw			SUM		
	45	90	135	45	90	135	45	90	135	45	90	135	45	90	135	45	90	135
NBrst	5	7	7	3	6	3	7	5	5	3	5	2	1	4	0	19	27	17
8k swp	0	1	0	1	4	4	6	6	6	3	5	2	3	3	1	13	19	13
TBrst	5	1	3	3	6	1	7	5	6	5	3	2	0	5	3	20	20	15
1,5Swp	1	4	7	3	4	3	5	6	5	4	3	1	1	5	1	14	22	17
Plses	5	3	6	0	3	2	4	4	6	3	3	1	2	4	1	14	17	16
sum	16	16	23	10	23	13	29	26	28	18	19	8	7	21	6			
																125	195	213

Table IV. Criterion Dispersions of Listeners, Icons, and Locations

ICON	*NBrst*	*8kSwp*	*TBrst*	*1.5kSw*	*Plses*			TOTAL	$\chi2$	
No. <30 Deg	55	18	41	44	37			195	18.29 w/	4 DF
%(N=105)	*52*	*17*	*39*	*42*	*35*		*%(Nt=525)*	*37*	α(.05)=9.49	
LISTENER	*rk*	*kb*	*mp*	*at*	*bw*					
No. <30 Deg	57	48	37	37	30			209	10.88 w/	4 DF
%(N=105)	*54*	*46*	*35*	*35*	*29*		*%(Nt=525)*	*40*	α(.05)=9.49	
AZIMUTH	*0*	*45*	*90*	*135*	*225*	*270*	*315*			
No. <30 Deg	37	37	41	26	22	26	6	195	30.78 w/	6DF
%(N=75)	*49*	*49*	*55*	*35*	*29*	*35*	*%(Nt=525)*	*37*	α(.05)=12.59	
ELEVATION	*45*	*90*	*135*						25.48 w/	2 DF
No. <30 Deg	31	86	62					179	α(.05)=5.99	
%(N=175)	*18*	*49*	*35*				*%(Nt=525)*	*34*		

Table V. Main Effects Analysis

Number of Criterion Responses

	Angle of Error	*rank*	Dispersion (1/k)	*rank*
rk	58	5	63	4
kb	51	4	45	2
mp	37	3	88	5
at	22	1	51	3
bw	26	2	41	1

Table VI. Relation of Angle of Error Versus Dispersion

6.0 SUMMARY

The overall hit rate for the number of responses (head-orientation) within the 30^0 angle of error for the criterion was about 37%. There were five listeners, and five icons presented at three elevations and seven azimuths for a total of 525 opportunities to match the target (after the test set averaging to calculate the angle of error and κ^{-1}). Table VII shows the number of observations in the various partitions. In the set of 525 there were 194 correct responses. Within the 194 correct head orientations, there were significant variations in the number of criterion target localizations. The χ^2 statistic was calculated for icon, listener, azimuth and elevation (Table IV) and all exceeded $\alpha_{(.05)}$. The icon with the broadest spectrum, the noise burst, elicited the largest number of localizations within the criterion. Within the test set, there were 105 opportunities for the noise burst to be correctly localized by the listeners, and 53% were within the criterion. Only 18% of the localizations of the 8 kHz Sweep icon were within the criterion angle of error. Surprisingly, the correct responses for the pulses icon was 32% while the 1.5 kHz Sweep elicited 42% correct. Most of these correct responses occurred for the horizontal elevation, i.e., 90°.

Only 23% of the responses to the 45° elevation were correct. The horizontal elevation was much more likely to elicit a correct reponse than either 45° elevation, up or down. Also curious was the occurrance of but 8% correct responses for the azimuth at 315°. In general the right side, i.e., 45° and 90°, were more accurately localized than the left side, i.e., 270° and 315°. The most accurately localized azimuth was 90° and not 0°, which might have been expected.

The significant χ^2 for listeners may hold some implication for subject selection. The two more effective listeners were male and the less effective were female. The female listeners did especially poorly on the two elevations. Table V shows the number of criterion responses for angle of error and dispersion for each listener. The ranks for angle of error and dispersion are dissimilar, indicating some dissociation between the two measures. Although the rank differences fall short of significance, they can imply that the perceptions, even though not agreeing with the target, were nevertheless precise and may indicate that the errors in location are due to inappropriate head related transfer functions for those listeners.

Numbers of Observations for Conditions

Experimental Condition		Number
Azimuth (45 deg. increments)		7
Elevation (45 deg. increments)		3
Icons		5
No. Observatioons/Run		105
Number of Listeners		5
Runs in Test Set		3
Total Number of Responses		1575
Test Set Averaging (3 Runs)		525
	Responses/Azim	75
Comparison Numbers	Responses/Elev	175
	Responses/Icon	105
	Responses/List.	105

Table VII. Number of Observations

7.0 CONCLUSIONS

In the Phase I effort, five acoustic signals were developed and presented to five listeners at seven azimuths and three elevations. Listeners could easily identify the signals but varied in their ability to localize them. The signals also differed in the variability and accuracy with which each listener localized them. The following conclusions summarize the Phase I research and provide a starting point for developing Phase II technical objectives.

1. Both spectral and temporal features of acoustic signals are important determiners of their efficacy for use as icons to indicate the location and nature of events. Even though the spectra of two signals may be similar with respect to power within a given frequency region, their temporal features may also contribute to the precision of their localization, and certainly to their recognition.

2. The differences among listeners, particularly with respect to estimating elevation, may be reduced by using Head Related Transfer Functions (HRTFs) measured for each listener. In Phase I the best performance occurred for signals presented at the horizon and the greatest error occurred for signals presented at -45^0, i.e., below the horizon. Since elevation is dependent on the configuration of the listener's external ear, the synthesis of virtual sources may be best when one's own HRTF is used.

3. The signal that showed the best localization was a broad band noise burst. Frequency representation was continuous for this signal from about 300 Hz to 10 kHz. Spectral measurements in the auditory canal (Wightman and Kistler, 1989a) show frequency/dependent variations in the 6-10 kHz frequency region as a function of speaker elevation. Although all signals were presented with abrupt rise times and, therefore, contained energy over a broad spectral range, the most prominent representation of frequencies in the 6-10 kHz frequency region occurred in the noise burst. The HRTFs capture the relation between elevation and frequency. When the signal has insufficient representation in the 6-10 kHz region, with respect to the energy below 3KHz, the listener is unable to resolve the virtual elevations.

REFERENCE

Wightman, F.L. & Kistler, D.J. (1989) Headphone simulation of free-field listening. II: Psychophysical validation, J. Acoust. Soc. Amer., 85 (2), pp. 868-878.

APPENDIX A

Data for Listener **RK**

Azimuth (ave. across elevation)

	NBrst	8kwp	TBrst	1.5 Sp	Plses
0	6	3	9	6	7
45	53	50	50	50	52
90	100	100	101	100	100
135	142	141	152	142	146
180					
225	231	231	240	232	234
270	277	277	283	278	278
315	326	324	324	322	326

Elev(ave acrss Az)

	NBrst	8kSwp	TBrst	1.5Sp	Plses
UP(45 DEG)	10.19	37.095	15.667	26.143	26.57143
HORIZ	-8.0952	-13.143	-13.762	-10.667	-15.52381
DWN(45 Deg)	-15.381	-17.048	-46.81	-16.857	-21.95238

Angle of Error for Azimuth

UP

	NBrst	8kSwp	TBrst	1.5Swp	Plses
0	6.62	67.89	11.16	46.93	42.30
45	11.67	49.24	8.62	40.46	21.66
90	16.88	40.51	11.09	14.18	10.47
135	10.45	55.72	36.85	44.68	12.09
225	30.96	51.53	55.44	39.23	41.88
270	19.13	39.23	42.11	43.32	57.55
315	23.43	80.74	10.45	66.31	36.91

HORIZ

	NBrst	8kSwp	TBrst	1.5Swp	Plses
0	3.91	46.99	25.20	16.52	16.40
45	11.04	32.35	26.40	22.33	20.10
90	19.63	33.38	24.02	24.31	26.60
135	14.51	39.57	52.99	23.52	18.14
225	11.49	33.58	37.46	10.47	34.89
270	12.07	12.32	50.57	20.83	30.57
315	36.38	77.89	52.28	60.75	60.09

DOWN

	NBrst	8kSwp	TBrst	1.5Swp	Plses
0	19.27	38.82	27.24	12.90	15.52
45	17.40	36.95	26.19	18.45	15.93
90	15.10	32.58	21.95	13.25	17.28
135	15.58	40.56	26.76	12.52	22.37
225	18.28	43.33	26.70	21.33	28.84
270	21.98	37.15	31.77	18.16	25.30
315	60.96	74.52	57.12	69.98	67.32

Variability (1/k

UP

	NBrst	8kSwp	TBrst	1.5Swp	Plses
0	0.002	0.771	0.004	0.556	0.363
45	0.011	0.318	0.013	0.212	0.073
90	0.082	0.393	0.012	0.044	0.011
135	0.022	0.639	0.233	0.433	0.009
225	0.138	0.268	0.061	0.118	0.019
270	0.038	0.096	0.171	0.239	0.087
315	0.087	0.786	0.003	0.801	0.008

HORIZ

	NBrst	8kSwp	TBrst	1.5Swp	Plses
0	0.001	0.708	0.137	0.029	0.025
45	0.003	0.150	0.072	0.099	0.055
90	0.003	0.111	0.160	0.084	0.106
135	0.001	0.497	0.457	0.033	0.052
225	0.003	0.265	0.196	0.009	0.360
270	0.022	0.007	0.767	0.048	0.287
315	0.003	1.087	0.083	0.710	0.750

DWN

	NBrst	8kSwp	TBrst	1.5Swp	Plses
0	0.026	0.282	0.063	0.006	0.019
45	0.022	0.251	0.113	0.006	0.019
90	0.009	0.232	0.094	0.014	0.003
135	0.025	0.262	0.083	0.020	0.061
225	0.022	0.286	0.067	0.016	0.044
270	0.003	0.169	0.111	0.003	0.009
315	0.009	0.320	0.004	0.012	0.760

Data for Listener **KB**

	NBrst	8kSwp	TBrst	1.5Sp	Plses
0	-1.44	0.33	-5.11	-7.11	-3.00
45	43.67	55.33	50.00	48.00	56.56
90	86.33	91.22	90.67	83.00	94.00
135	130.56	129.00	130.11	128.67	130.00
180					
225	229.78	234.11	238.56	230.22	236.61
270	269.78	268.22	272.11	268.22	279.00
315	311.50	308.22	303.44	312.44	322.33

Elev Error (ave. acrss Az)

	NBrst	8kSwp	TBrst	1.5Sp	Plses
UP(45 Deg)	51.00	39.24	41.86	46.57	51.76
HORIZ	0.52	-19.86	-0.14	-3.48	-10.52
DWN(45 Deg)	-24.67	-33.38	-30.86	-23.33	-24.21

Angle of Error for Azimuth

UP

	NBrst	8kSwp	TBrst	1.5Sp	Plses
0	47.575	38.724	34.778	11.873	30.095
45	35.575	34.867	24.77	31.231	24.124
90	42.019	31.673	38.091	40.809	34.112
135	40.288	41.816	32.343	27.308	29.315
225	31.316	35.497	35.616	34.185	23.656
270	40.801	33.37	27.881	27.091	54.692
315	35.877	33.575	28.205	22.068	71.336

HORIZ

	NBrst	8kSwp	TBrst	1.5Sp	Plses
0	23.054	50.926	12.493	28.209	22.839
45	9.3563	19.701	17.993	28.135	35.471
90	7.8893	19.048	18.166	18.675	14.739
135	19.731	51.637	28.351	34.788	8.1392
225	26.437	48.33	14.732	13.297	70.836
270	31.63	16.895	26.476	16.855	48.24
315	51.098	53.623	57.272	51.886	76.205

DWN

	NBrst	8kSwp	TBrst	1.5Sp	Plses
0	24.932	15.714	21.928	28.436	34.225
45	33.126	42.789	30.692	25.396	29.198
90	25.343	25.828	27.288	14.299	23.201
135	22.246	32.215	34.693	30.043	29.87
225	13.119	36.774	42.058	20.629	12.937
270	23.12	28.756	38.312	19.247	50.307
315	85.515	73.09	72.544	63.609	87.859

Variability (1/k)

UP

	NBrst	8kSwp	TBrst	1.5Sp	Plses
0	0.2229	0.3541	0.0761	0.0024	0.2682
45	0.1239	0.1003	0.1799	0.3077	0.1923
90	0.0179	0.2822	0.4411	0.0126	0.3784
135	0.4021	0.5153	0.0522	0.1614	0.285
225	0.3191	0.3649	0.4039	0.0708	0.1735
270	0.077	0.0751	0.0432	0.2371	0.8318
315	0.0344	0.3019	0.1965	0.1234	

HORIZ

	NBrst	8kSwp	TBrst	1.5Sp	Plses
0	0.0042	0.7858	0.015	0.1077	0.034
45	0.0111	0.095	0.0709	0.0216	0.1442
90	0.0102	0.0042	0.0759	0.0376	0.0325
135	0.0282	0.4738	0.1129	0.1032	0.0042
225	0.1068	0.7502	0.0101	0.013	1.1179
270	0.037	0.043	0.0631	0.0238	0.7501
315	0.0164	0.0151	0.0479	0.1156	

DWN

	NBrst	8kSwp	TBrst	1.5Sp	Plses
0	0.1013	0.0248	0.1128	0.113	0.3597
45	0.1895	0.1483	0.2313	0.1484	0.2172
90	0.0329	0.0891	0.2498	0.0092	0.0942
135	0.062	0.1769	0.0433	0.2964	0.2656
225	0.0189	0.09	0.4719	0.0666	0.0204
270	0.1018	0.2533	0.4687	0.0493	0.7774
315	0.7619	0.0798	0.3375	0.4155	

Data for Listener **MP**

	NBrst	8kwp	TBrst	1.5 Sp	Plses
0	-1	3	7	-3	-1
45	43	40	37	38	36
90	93	81	85	83	77
135	145	110	98	130	109
180					
225	240	250	252	249	243
270	274	276	287	282	279
315	273	323	293	327	309

Elev(ave acrss Az)

	NBrst	8kSwp	TBrst	1.5Sp	Plses
UP(45)	51.095	38.048	41.143	45.238	36.19
HORIZ	1.619	-3.8095	-2.4286	-6.0476	-10.389
DWN(45)	-28.048	-43.81	-47.143	-43.333	-48.667

up — Error for Azimuth

	NBrst	8kSwp	TBrst	1.5Swp	Plses
0	27.771	67.688	34.367	42.064	67.578
45	46.278	40.131	34.577	55.366	25.853
90	32.295	40.683	61.41	55.239	63.567
135	15.146	36.617	48.592	66.356	54.64
225	18.467	47.368	45.035	79.577	48.499
270	43.258	52.358	57.191	77.465	46.752
315	57.559	47.735	31.866	51.221	50.917

up — 1/k

	NBrst	8kSwp	TBrst	1.5Swp	Plses
0	0.0004	0.0304	0.0341	5E-05	0.0022
45	0.036	0.1471	0.0665	0.0093	0.1202
90	0.0517	0.0006	0.0146	0.1111	3E-05
135	0.0026	0.0017	0.011	0.0402	0.0078
225	0.0047	0.0046	0.0707	0.002	0.1429
270	0.0879	0.0151	0.0587	0.106	0.0009
315	0.0062	0.0628	0.005	0.002	0.5962

Horiz

	NBrst	8kSwp	TBrst	1.5Swp	Plses
0	19.951	25.241	19.032	6.6354	2.4503
45	11.423	15.78	28.23	14.499	19.362
90	18.979	24.008	13.712	17.515	28.706
135	99.754	50.111	23.212	24.343	33.444
225	24.476	33.949	36.143	36.374	
270	30.257	19.386	11.831	13.596	13.873
315	53.445	39.401	40.03	27.226	

Horiz

	NBrst	8kSwp	TBrst	1.5Swp	Plses
0	0.0134	0.0637	0.0285	0.001	0.0002
45	0.0183	0.0201	0.0677	0.0108	0.0046
90	0.0036	0.0352	0.0027	0.0507	0.0753
135	0.9216	0.75	0.1196	0.1407	0.0882
225	0.0093	0.0152	0.1443	0.0007	
270	0.0603	0.0345	0.032	0.0292	0.0502
315	0.0814	0.0015	0.0102	0.014	

down

	NBrst	8kSwp	TBrst	1.5Swp	Plses
0	43.743	39.712	21.958	28.701	37.335
45	28.006	35.632	31.48	41.544	25.055
90	23.758	38.725	29.79	26.14	41.393
135	27.244	57.912	55.124	40.929	52.791
225	23.731	47.118	42.327	49.928	43.086
270	21.95	37.447	36.72	49.791	50.274
315	84.474	71.878	78.411	89.544	94.655

DWN

	NBrst	8kSwp	TBrst	1.5Swp	Plses
0	0.002	0.0164	0.0061	0.036	0.0165
45	0.0963	0.0409	0.0721	0.011	0.0169
90	0.1024	0.1064	0.0162	0.0929	0.0003
135	0.0154	0.0437	0.1578	0.0309	0.0456
225	0.0078	0.0643	0.023	0.051	0.0723
270	0.0311	0.0776	0.0342	0.1114	0.0257
315	0.0227	0.0164	0.0471	0.0128	0.75

Data for Listener **AT**

	NBrst	8kSwp	TBrst	1.5Sp	Plses
0	19.333	10.889	8.5556	7.7778	54.111
45	42.778	69.222	50.667	91.222	79.444
90	106.89	113.22	105.11	112.11	100.44
135	178.11	172.89	151.11	173.22	145
180					
225	252.44	228	258.11	231.44	253.44
270	275.67	285.06	250.56	271.17	293.56
315	287.33	335	266.89	329.67	208

Elev(ave acrss Az)

	NBrst	8kSwp	TBrst	1.5Sp	Plses
UP(45 Deg)	37	26.381	24.905	28.667	18.143
HORIZ	-20.381	-20.81	-27.381	-21.381	-12.619
DWN(45 Deg)	-17.476	-24.762	-42.143	-34.619	-21.167

Angle of Error for Azimuth

UP

	NBrst	8kSwp	TBrst	1.5Sp	Plses
0	20.14	70.191	21.916	65.012	82.798
45	57.229	69.291	19.978	58.366	22.882
90	74.009	16.809	81.257	57.845	85.472
135	40.589	36.558	43.235	57.939	58.948
225	49.178	56.23	43.912	40.673	43.473
270	23.877	40.161	40.193	16.827	70.47
315	45.972	76.068	58.726	77.877	81.831

HORIZ

	NBrst	8kSwp	TBrst	1.5Sp	Plses
0	28.492	32.668	36.57	36.663	39.298
45	37.415	43.114	48.637	68.347	25.241
90	37.738	41.86	41.453	35.069	39.88
135	55.366	46.425	45.599	59.377	50.455
225	11.541	29.164	26.76	27.01	30.004
270	41.47	43.14	32.043	36.093	38.394
315	25.413	30.915	39.02	36.783	78.456

DWN

	NBrst	8kSwp	TBrst	1.5Sp	Plses
0	27.182	22.524	31.741	26.634	33.492
45	29.851	41.19	30.476	37.926	27.242
90	26.373	31.464	27.821	42.143	29.682
135	49.275	51.561	43.624	38.842	32.998
225	37.909	36.183	35.555	36.597	40.512
270	51.668	50.211	62.164	50.477	56.73
315	53.706	66.198	36.357	69.881	41.895

1/k

UP

	NBrst	8kSwp	TBrst	1.5Sp	Plses
0	0.0106	0.0546	0.076	0.022	0.0031
45	0.4451	0.4476	0.054	0.435	0.0283
90	0.5219	0.0121	0.025	0.4186	0.1171
135	0.017	0.1443	0.025	0.3508	0.4133
225	0.2211	0.1741	0.047	0.0775	0.048
270	0.0634	0.3155	0.416	0.0178	0.102
315	0.4443	0.003	0.312	0.0232	

HORIZ

	NBrst	8kSwp	TBrst	1.5Sp	Plses
0	0.0495	0.0837	0.041	0.1073	0.085
45	0.0291	0.0614	0.254	0.8393	0.0146
90	0.0957	0.0339	0.022	0.02	0.1162
135	0.1476	0.1185	0.485	0.0968	0.197
225	0.0131	0.0668	0.149	0.0949	0.0976
270	0.0499	0.0786	0.11	0.0265	0.0407
315	0.0191	0.0643	0.01	0.0756	

DWN

	NBrst	8kSwp	TBrst	1.5Sp	Plses
0	0.0194	0.0541	0.036	0.2114	0.3439
45	0.2958	0.3495	0.223	0.2554	0.2292
90	0.1945	0.1848	0.153	0.3529	0.1384
135	0.0223	0.0427	0.215	0.0859	0.151
225	0.2507	0.179	0.134	0.1001	0.0382
270	0.8318	0.7985	1.121	0.7737	0.9707
315	0.2781	0.5047	0.038	0.4623	0.1931

Data for Listener **BW**

	NBrst	8kSwp	TBrst	1.5Swp	Plses
0	2.22	4.67	3.56	36.00	0.00
45	42.11	45.11	32.44	40.22	36.11
90	78.67	80.11	69.78	72.89	69.78
135	119.78	110.89	118.67	110.78	104.00
180					
225	170.67	210.22	198.78	227.44	244.89
270	287.33	291.89	304.33	251.33	282.67
315	296.44	219.22	261.00	218.22	289.44

Elev (ave acrss Az)

	NBrst	8kSwp	TBrst	1.5Sp	Plses
UP(45 Deg)	28.81	35.00	39.52	38.14	41.72
HORIZ	-6.43	-6.38	-4.81	-11.05	-11.67
DWN(45 Deg)	-17.00	-30.62	-41.05	-31.33	-30.62

Angle of Error for Azimuth

UP

	NBrst	8kSwp	TBrst	1.5Swp	Plses
0	34.827	41.643	39.176	43.774	44.241
45	33.046	21.881	37.805	30.939	39.362
90	24.198	31.311	19.489	42.3	40.767
135	27.567	38.517	37.662	36.007	39.897
225	76.144	98.803	74.181	45.194	55.573
270	33.104	65.764	55.704	39.589	39.982
315	46.459	50.696	53.726	36.595	35.427

HORIZ

	NBrst	8kSwp	TBrst	1.5Swp	Plses
0	32.773	47.572	21.346	18.272	9.4683
45	44.864	15.448	25.262	26.098	26.824
90	42.139	14.668	21.409	23.435	30.881
135	18.603	19.964	19.878	27.029	24.566
225	22.618	33.301	24.142	31.561	33.511
270	15.827	10.392	13.959	16.775	21.089
315	39.516	57.228	43.029	49.007	76.135

DWN

	NBrst	8kSwp	TBrst	1.5Swp	Plses
0	28.111	43.05	35.79	40.233	44.051
45	54.164	56.874	49.494	54.382	39.618
90	24.153	67.523	63.184	29.048	46.663
135	21.618	44.349	52.679	53.451	52.322
225	72.633	73.297	73.578	51.096	97.536
270	48.202	39.422	74.117	55.517	53.429
315	56.222	43.261	55.669	35.427	73.762

1/k

UP

	NBrst	8kSwp	TBrst	1.5Swp	Plses
0	0.1231	0.063	0.2891	0.558	0.009
45	0.8265	0.0407	0.4043	0.0742	0.0519
90	0.1652	0.0248	0.0708	0.1049	0.1075
135	0.2026	0.1171	0.3063	0.2396	0.2726
225	0.8108	0.6713	1.2165	0.4685	0.5869
270	0.0867	0.415	0.4964	0.4771	0.3683
315	0.1539	0.0735	0.1951	0.2213	

HORIZ

	NBrst	8kSwp	TBrst	1.5Swp	Plses
0	0.26	0.2424	0.0893	0.0639	0.0167
45	0.5856	0.042	0.0756	0.0199	0.0089
90	0.0991	0.0286	0.0548	0.0255	0.1835
135	0.0197	0.1058	0.0502	0.1111	0.1853
225	0.0774	0.0927	0.0149	0.0745	0.0671
270	0.0365	0.0141	0.014	0.0162	0.0594
315	0.2995	0.2567	0.1873	0.1332	

DWN

	NBrst	8kSwp	TBrst	1.5Swp	Plses
0	0.1652	0.0047	0.2318	0.061	0.0613
45	0.6392	0.4249	0.0055	0.5281	0.3607
90	0.1766	0.2071	0.0884	0.1155	0.4181
135	0.0669	0.2352	0.5664	0.3968	0.4322
225	1.1196	0.7595	0.9885	0.201	0.3371
270	0.2901	0.2115	0.0359	0.1073	0.1269
315	0.2292	0.123	0.2045	0.1427	0.3945

APPENDIX B

The procedure used to calculate the vector quantities, angle of error and κ^{-1}, follow the description by Wightman and Kistler (1989). However, the description below was worked out here. Any errors are ours and may not be attributed to anyone else.

Angle of Error

The analysis of the listeners' head-orientations, read from the iso-tracker, were in degrees azimuth and degrees elevation. Head gaze forward was 0^0,90^0, according to the coordinates used for the 3DAG. Thus, 90^0 azimuth was to the right of the listener, roughly opposite the right ear, and 270^0 was to the left, roughly opposite the left ear. In the median plane, 0^0 was directly above the listener's head and 180^0 was directly below the listener. Our stimuli were presented at 45^0 degree increments in azimuth, i.e., there were seven azimuth angles (excluding 180^0) and in elevation (45^0, 90^0, and 135^0), for a total of 21 virtual source locations for each of the five icons for each run.

The angle of error was the difference, in vector terms, of the mean of three runs and the target vector for each angle. The x, y, z coordinates of the target location were determined from the sine and cosine values of the angle in azimuth and elevation.

x= (cos azimuth angle)(cos elevation angle)
y= (sin elevation angle)
z= (sin azimuth angle)(cos elevation angle)

The x, y and z coordinates for each angle indicated by the head-orientation readings were also determined. The mean values of the coordinates were calculated for the three test runs, taken after approximately 24-30 hours of scheduled practice.

The difference between the two angles, target and response, is determined from the arc cosine of the dot products for each pair of angles,

$$D= \arc\cos (x_R \quad x_T) + (y_R \quad y_T) + (z_R \quad z_T)$$

where xt, yt, zt represent the coordinates for the target angle and x_R, y_R, z_R represent the coordinates of the response angle to that target for each listener.

Variability (κ^{-1})

Wightman and Kistler (1989) discuss the problem of describing the variability of judgements in spherical coordinates, citing the von Mises-Fisher distribution, k (kappa). These authors cite Fisher, Lewis and Embleton (1987) as the source for an unbiased estimate of κ , as

$$\kappa' = (N-1)2 / N(N-R),$$

where N= number of observations (note: less than 16)
R= the length of the judgement vector.

In the sense of spherical coordinates, Wightman & Kistler (1989) speak of the "dispersion" of the judgements about the inner surface of the sphere. An important quantity that must be calculated from the judgement vectors is the length of the resultant. The length of the resultant is calculated by the relation,

$$R = \sqrt{\left(\sum x_r\right)^2} + \sqrt{\left(\sum y_r\right)^2} + \sqrt{\left(\sum z_r\right)^2}$$

If each member of the set of responses is a perfect match to the target, the dispersion is low and R, the length of the vector, approaches N and k becomes very large. Wightman and Kistler (1989) state that κ^{-1} is the conventional expression used to describe dispersion in spherical coordinates and that is what we have calculated to describe the present data set. Note that there is a κ^{-1} for each of the 21 target angles, calculated for the set of 3 test runs. That is, for our study, N=3 in the equation for the estimate of κ.